Adsorptive removal of acetamiprid pesticide from aqueous solution using environmentally friendly natural and agricultural wastes

Somaia G. Mohammad[a,*], Sahar M. Ahmed[b]

[a]*Central Agricultural Pesticides Laboratory, Pesticide Residues and Environmental Pollution Department, Agriculture Research Center (ARC), 12618, Dokki, Giza, Egypt, Fax +20- 3 7602209, email: somaiagaber@yahoo.com, sommohammad2015@gmail.com (S.G. Mohammad)*
[b]*Egyptian Petroleum Research Institute, Nasr City, Cairo, Egypt, Fax +20 2 2274 7433, email: saharahmed92@hotmail (S.M. Ahmed)*

ABSTRACT

The potentiality of eco-friendly low cost natural and agricultural wastes of orange peels (OPAC) and almond shells (ASAC) prepared for the removal of acetamiprid pesticide from aqueous solution has been investigated in batch experiments. Structure and morphology of OPAC and ASAC were characterized by Fourier transform infrared spectroscopy (FTIR), x-ray diffraction (XRD), Field Emission scanning electron microscopy equipped with an energy dispersive x-ray analyzer (SEM-EDX) and surface area (BET) was determined by the nitrogen adsorption and desorption isotherm. The effect of various physicochemical parameters such as initial acetamiprid concentrations, adsorbent dose and contact time has been studied. The percent removal of acetamiprid onto OPAC and ASAC were 99.46 and 99.45% from aqueous solutions. The adsorption process was attained an equilibrium within 120 min of contact time. The experimental isotherms data were analyzed using Freundlich, Langmuir, and Dubinin-Radushkvich (D-R) isotherm equations. Results showed that adsorption isotherms of acetamiprid onto OPAC and ASAC can be slightly better- fitted data by the Freundlich model than Langmuir model. The maximum adsorption capacities were 151.515 and 370.37 mg g^{-1} for OPAC and ASAC, respectively. The energy of adsorption for OPAC and ASAC were 0.791 and 0.845 KJ/mol, indicating that the adsorption process is physical in nature. The kinetic adsorption of acetamiprid was fitted well the pseudo-second-order kinetic model for OPAC and ASAC, respectively.

Keywords: Activated carbon; Almond shell; Orange peel; Removal; Acetamiprid; Pesticide

1. Introduction

Pollution of surface and ground waters causes risk to human health in the case of the potential health hazards of their constituents of inorganic and organic compounds. Pesticides are like hazardous compounds that cause water pollution due to their extensive application for insecticides, acaricides, repellants, fungicides, herbicides, etc. The common usage of these chemicals has some undesirable effects such as toxicity, carcinocity and mutagenity [1–3].

Among the numerous agrochemicals, acetamiprid, a neonicotinoid insecticide, is a nitromethylene heterocyclic compound that has a relatively strong groundwater infiltra-tion [4]. Acetamiprid has been widely used in agriculture because of its good insecticidal effect. It shows excellent efficacy against aphids, leafhoppers, whiteflies, thrips etc. in various crops like okra, mustard, strawberry, cotton, and citrus. But it has also brought serious environmental problems at the same time [5], due to the high stability and solubility of acetamiprid in aqueous solution [6]. Recently, acetamiprid residues in the environment have received considerable attention due to their potential toxicity to humans. Therefore, it is important to prevent the accumulation of acetamiprid in the environment

There are several procedures available for pesticides removal from water which includes photocatalytic degradation [7,8], ultrasound combined with photo-Fenton

*Corresponding author.

treatment [9], advanced oxidation processes [10], ozonation [11] and adsorption [12]. Adsorption by activated carbon (AC) is one of the most widely used techniques and has proven to be effective in the removal of pesticides [13], heavy metals [14,15], dyes [16–19] and phenols from aqueous solutions.

Activated carbons (ACs) are porous materials that have a high surface area and high adsorption capacity, which can remove a wide variety of pollutants such as dyes, heavy metals, pesticides, and gases. Due to its adsorptive properties, the ACs are used to purify, detoxify, deodorize, filter, discolor or alter the concentration of many liquid and gaseous materials. These applications are of great interest in various industrial sectors such as food, pharmaceutical, chemical, oil, mining, and especially in the treatment of drinking water [20]. Because of the high cost and non-renewable source of commercially available AC, in recent years, researchers have studied the production of ACs from cheap and renewable precursors, such as olive husk [21] and cotton stalks [22].

Among the agricultural wastes, orange, as a kind of biological resources is available in large quantities in many parts of the world. The use of orange peel as a biosorbent material presents strong potential due to its main components of cellulose, pectin (galacturonic acid), hemicellulose and lignin. These components bear various polar functional groups including carboxylic and phenolic acid groups [23–25]. As a low cost, orange peel is an attractive and inexpensive option for the biosorption removal of dissolved metals. Some authors reported the use of orange waste as a precursor material for the preparation of an adsorbent by common chemical modifications such as alkaline, acid, ethanol and acetone treatment [26].

Almond (*Prunus amygdalus L.*) is one of the important agricultural materials, abundant, effective and cheap. It is cultivated in some countries such as USA, Spain, Morocco, Iran, and Turkey, and is globally consumed. When the fruit of almond is processed to obtain the edible seed, big ligneous shell fragments are separated. Almond shells can be used as an adsorbent. The cell walls of almond shell consist of cellulose, silica, lignin, and carbohydrates which have hydroxyl groups in their structures [27–29]. These materials cause potential disposal problems since they exist in enormous quantities, and have no important practical utility [30].

To the best of our knowledge, there is no any study devoted to the potential applicability of for the removal of pesticide acetamiprid by two different kinds of activated carbon from two different agricultural wastes orange peels and almond shells as precursors and low cost adsorbents from aqueous solution. Some researcher, Fatima and Belkacem (2016) prepared activated carbon from natural clay and used it as a cheap adsorbent for removal of acetamiprid from aqueous solution [31].

The use of agricultural wastes as the precursor for the preparation of activated carbons will provide the solution to environmental problems caused by wastes as well as they produce benefit products from low cost materials. Therefore, the main objectives of this study were to investigate the potentiality of using inexpensive agricultural wastes (cellulose based wastes), Orange Peels Activated Carbon (OPAC) and Almond Sells Activated Carbon (ASAC) as

an adsorbent for the removal of acetamiprid. The effects of adsorbent mass, initial pesticide concentrations and contact time on acetamiprid removal were studied. Adsorption isotherms and kinetics parameters were also calculated and discussed.

2. Materials and methods

2.1. Chemicals

Physico-chemical properties of acetamiprid pesticide are reported in Table 1. All reagents used in this study were of analytical grade. Before each experiment, all glassware was cleaned with dilute nitric acid and repeatedly washed with deionized water.
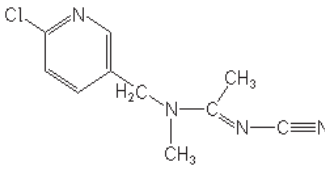
2.2. Equipment

The concentration of acetamiprid pesticide was determined by Agilent HPLC 1260 infinity series (Agilent Technologies) equipped with a quaternary pump, a variable wavelength diode array detector (DAD). Quanta 250 FEG (Field Emission Gun) scanning electron microscopy (Netherlands) was used for scanning the adsorbent surface attached with EDX Unit (Energy Dispersive X-ray Analyses), with accelerating voltage 30 KV. The infrared spectra of adsorbents were recorded in KBr discs on an infrared spectrophotometer (Model PerkinElmer 1720). XRD patterns were recorded on a Pan Analytical model X'Pert Pro (Almelo, Netherlands) with Cu Ka radiation (1.54 A°) at 40 kV and 40 mA in the 2θ range 10–80. Deionized water was prepared using a Millipore Milli-Q (Bedford, MA) water purification system. The Brunauere Emmette Teller (BET) surface area (SBET) for OPAC and ASAC was determined by the nitrogen adsorption and desorption isotherm, pore size distribution and specific surface area were measured using an AUTOSORB-1 surface area and pore size analyzer at 77 K.

2.3. Preparation of the adsorbent

Orange peels (OP) were collected from a local fruit in Egypt. Almond shells (AS) were collected from a local center of preparation of shell-removed almond in Egypt. Orange

Table 1
Some properties and chemical structure of acetamiprid

Common name	Acetamiprid
Chemical structure	
Pesticide group	Neonicotinoid Insecticide
Molecular formula	$C_{10}H_{11}ClN_4$
Molecular weight (g·mol^{-1})	222.68
Pesticide Type	Insecticide
Solubility in water (mg L^{-1})	4250 mg/L

peels and almond shells were cut into small pieces and, after drying and crushing, washed thoroughly with double-distilled water to remove adhering dirt. Then, they were dried in an oven at 100ºC for 24 h and were sieved. The sample was then soaked in orthophosphoric acid (H_3PO_4) with an impregnation ratio of 1:1 (w/w) for 24 h and dehydrated in an oven overnight at 105ºC. The resultant sample was activated in a closed muffle furnace to increase the surface area at 500ºC for 2 h. The AC produced was cooled to room temperature and washed with 0.1 M HCl and successively with distilled water. Washing with distilled water was done repeatedly until the pH of the filtrate reached 6–7. The final product was dried in an oven at 105ºC for 24 h and stored in a vacuum desiccator until needed [32].

2.4. Adsorption experiments

The adsorption experiments of acetamiprid onto OPAC and ASAC were carried out in a set of 150 Erlenmeyer flasks. 100 ml of the pesticide solutions of various initial concentrations in the range 100–800 mgL⁻¹ were added to separate flasks and a fixed dose of (1 g for OPAC and 0.5 g for ASAC) were added to each flask covered with glass stopper at room temperature (25ºC ± 2) with occasional agitation to reach equilibrium.

For kinetic studies of acetamiprid onto OPAC and ASAC, 100 ml of the solution containing 1000 mg/L with 1 g of OPAC and 0.5 g of ASAC for different time intervals from 5 to 180 min to determine the equilibrium time at room temperature (25ºC ± 2).

Isothermal studies of acetamiprid were conducted with an adsorbent quantity of 1 g for OPAC and 0.5 g ASAC with acetamiprid concentrations of 100, 200, 300, 400, 500, 600, 700 and 800 mg/L in identical conical flasks. Blank solutions were treated similarly (without adsorbent).

All samples should be cleaned by filtration with Target Nylon (0.45 µm) prior to analysis in order to minimize the interference of the carbon fines with the analysis. The samples were analyzed using HPLC with DAD.

The adsorption capacity was determined by using the following equation, taking into account the concentration difference of the solution at the beginning and at equilibrium [33].

$$q_e = \frac{(C_0 - C_e)}{m} \tag{1}$$

where C_0 and C_e are the initial and the equilibrium concentration of acetamiprid mg/L, respectively, V is the volume of solution (ml) and m is the amount of adsorbent used (g). The removal percent of acetamiprid from solution was calculated by the following equation:

$$Removal(\%) = \frac{(C_0 - C_e)V}{m} \tag{2}$$

2.5. HPLC analysis

The concentrations of acetamiprid in the solutions before and after adsorption were determined using an Agilent HPLC 1260 infinity series (Agilent technologies) equipped with a quaternary pump, a variable wavelength diode array detector (DAD) and an auto-sampler with an electric sample valve. The column was Nucleosil C_{18} (30 × 4.6 mm (i.d) × 5 µm) film thickness. The mobile phase was 30/70 (V/V) mixture of HPLC grade acetonitrile/water. The mobile phase flow rate was 1 ml/min. The wavelength was 246 nm. The retention time of acetamiprid was 6.1 min and the injection volume was 5 µL under the conditions.

3. Results and discussion

3.1. Characterization of the prepared adsorbents (OPAC and ASAC).

Scanning electron micrograph (SEM) images of the prepared OPAC and ASAC before and after adsorption are shown in Figs. 1 and 2, respectively. The SEM images obviously are shown the porous nature of prepared active carbons from AS and OP. The OPAC has holes and cave type opening on its surface and that accessible more surface area available for adsorption of acetamiprid [34]. After
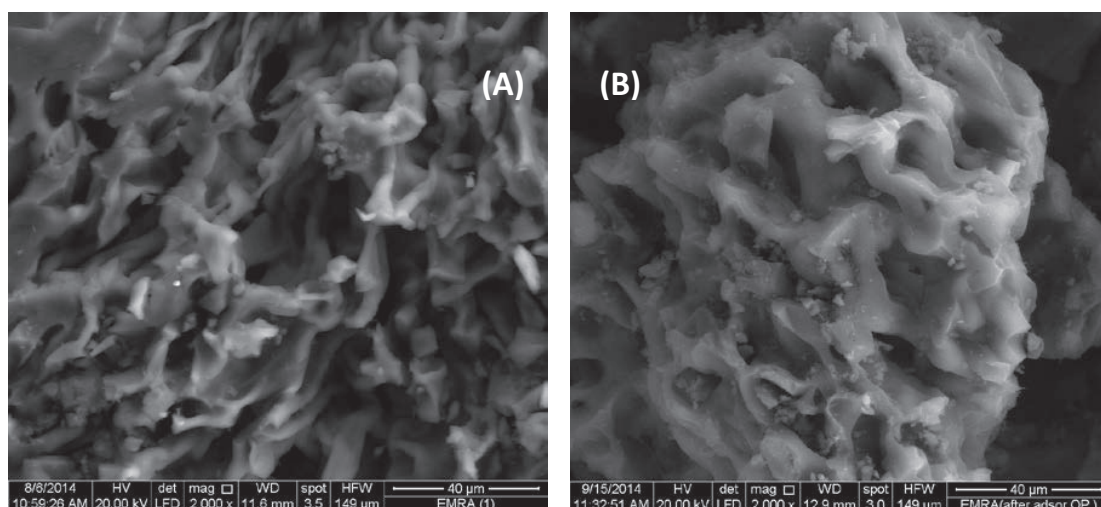

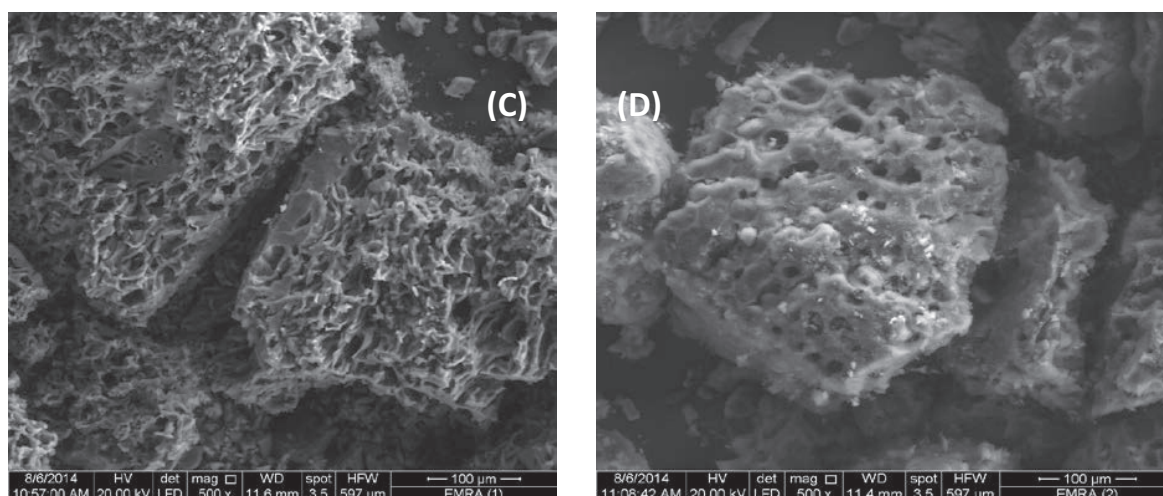Fig. 1. SEM images of OPAC (A) before adsorption of acetamiprid (B) after adsorption.

Fig. 2. SEM images of ASAC (C) before adsorption of acetamiprid (D) after adsorption.

adsorption of pesticide, change is observed in the structure of the OPAC due to covering partially by the acetamiprid pesticide molecules. Meanwhile, the prepared ASAC sample presents an irregular and a large number of micropores of various sizes at the surface. The availability of pores and internal surface is clearly displayed in the SEM picture of the prepared samples before adsorption and the coverage of the surface and the pores by the adsorbed pesticide is shown in Fig. 2. The pore formation of activated carbon is mainly attributed to the addition of phosphoric acid which causes the samples to swell and it opens the surface structure.

It has been reported that H_3PO_4 accelerated the bond cleavage reactions leading to the early evolution of volatiles at below 300°C and generation of empty spaces. At high temperatures, the reactive sites leave a hard aromatic carbon porous structure for adsorption [35].

In order to know the composition of OPAC and ASAC, elemental analysis was done using of EDX analysis. The EDX analysis is shown in Fig. 3 which show the presence of various elements such as Ca, Al, P in the very small percentage. They not play any role with the used pesticide acetamiprid and high amount of carbon 73.75% and 62.98% for OPAC and ASAC, respectively [36]. The active sites and porosity of the prepared activated carbon plays the main role in the adsorption process.

FTIR spectra of the prepared ASAC and OPAC are shown in Fig. 4. ASAC spectrum (Fig. 4A) is shown a broad peak in the range of 3200–3600 cm^{-1} with a maximum at about 3384 cm^{-1} is assigned to the O-H stretching mode of hydroxyl groups and adsorbed water. A medium band of symmetric and asymmetric C-H stretching vibration at 2941 and 2892 cm^{-1} is due to the presence of methyl group on the surface. The peak observed at 1738 cm^{-1} is the stretching vibration of a bond due to carboxyl groups and may be assigned to carboxylic acids or their esters. A strong absorption at 1235 cm^{-1} is for C-O stretch due to an alcoholic group and a strong absorption at 1627 cm^{-1} is due to C–C stretch. The peaks around 1418 cm^{-1} are due to the symmetric bending of CH$_3$. The peak observed at 1020 cm^{-1} is attributed to C–H in the plane [37]. FTIR spectrum of OPAC is shown in Fig. 4b. The broad and intense adsorption peaks at around
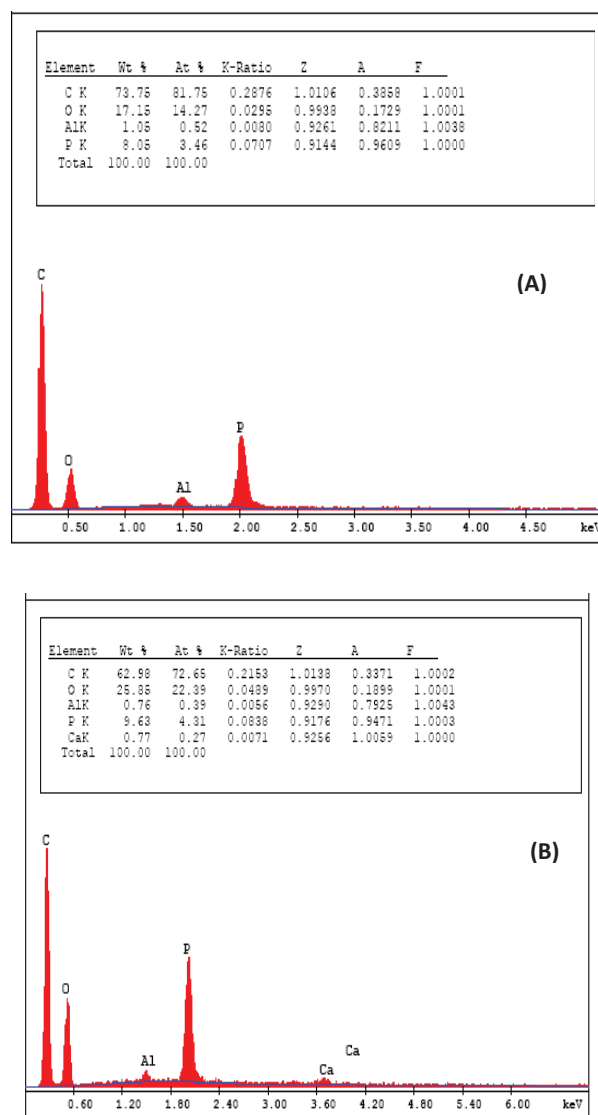

Element	Wt %	At %	K-Ratio	Z	A	F
C K	73.75	81.75	0.2876	1.0106	0.3858	1.0001
O K	17.15	14.27	0.0295	0.9938	0.1729	1.0001
AlK	1.05	0.52	0.0080	0.9261	0.8211	1.0038
P K	8.05	3.46	0.0707	0.9144	0.9609	1.0000
Total	100.00	100.00				

(A)

Element	Wt %	At %	K-Ratio	Z	A	F
C K	62.98	72.65	0.2153	1.0138	0.3371	1.0002
O K	25.86	22.39	0.0489	0.9970	0.1899	1.0001
AlK	0.76	0.39	0.0056	0.9290	0.7925	1.0043
P K	9.63	4.31	0.0838	0.9176	0.9471	1.0003
CaK	0.77	0.27	0.0071	0.9256	1.0059	1.0000
Total	100.00	100.00				

(B)

Fig. 3. EDX spectra of (A) OPAC (B) ASAC.

3384 cm⁻¹ correspond to O–H stretching vibrations. The peaks at 2928 and 2874 cm⁻¹ are attributed to the symmetric and asymmetric C–H stretching vibration of aliphatic acids. The peak observed at 1709 cm⁻¹ is the stretching vibration of bond carboxyl groups and may be assigned to carboxylic acids or their esters. The peak observed at 1608 cm⁻¹ is due to C=C stretching that can be attributed to the aromatic C–C

bond. Beside appearance of a weak bond at 670 cm⁻¹ for Ca phosphate.

XRD patterns for the prepared activated carbon OPAC and ASAC are shown in Fig. 5. It has been observed two peaks at 2θ = 25.18 and 45.8 attributed d_{002} and d_{100}, respectively. These diffraction peaks are evidence that the samples have a turbostratic structure. This turbostratic model assumes that the samples are made of graphite-like microcrystallites, bounded by cross-linking network, consisting of several graphite-like layers [38]. The value of d_{002} is comparable with those reported by Kumar et al. on activated carbon cloth [39].

3.1.1. BET surface area and pore characteristics

Figs. 6 and 7 show N_2 adsorption-desorption isotherms and pore-size distribution curves of orange peel active carbon and almond shell active carbon. As seen in Figs. 6 and 7, according to analyzing adsorption characteristics of activated carbons from the OPAC, it was found that it had the characteristics of type I adsorption isotherm. On the other hand, ASAC shows a combination of type I and IV isotherm curves. This is indicating the existence of micropores and mesopores in the ASAC structure, also the N_2 adsorbed increased sharply when the value of P/P_o was low the nit increases gradually as the pressure increases. The specific surface area of ASAC activated carbon and OPAC activated carbon are 1147 m²/g and 174.4 m²/g, respectively. The total pore volume for pores with Diameter less than 291.13 nm at P/P_o = 0.993378 was 0.8330 cc/g for ASAC and the total pore volume for pores with diameter less than 251.69 nm at P/P_o = 0.992329 was 0.02765 cc/g for OPAC. According to t-plot method, the external surface area is 375.1 m²/g and micropore surface area is 771.5 m²/g for ASAC, meanwhile the external surface area is 20.53 m²/g and micropore surface area is 153.9 m²/g for OPAC. The pore size of ASAC and OPAC was mainly in the 2–4 nm range. Therefore, the structure of ASAC and OPAC was a combination of meso- and micro-pores with a larger proportion of mesopores [40].
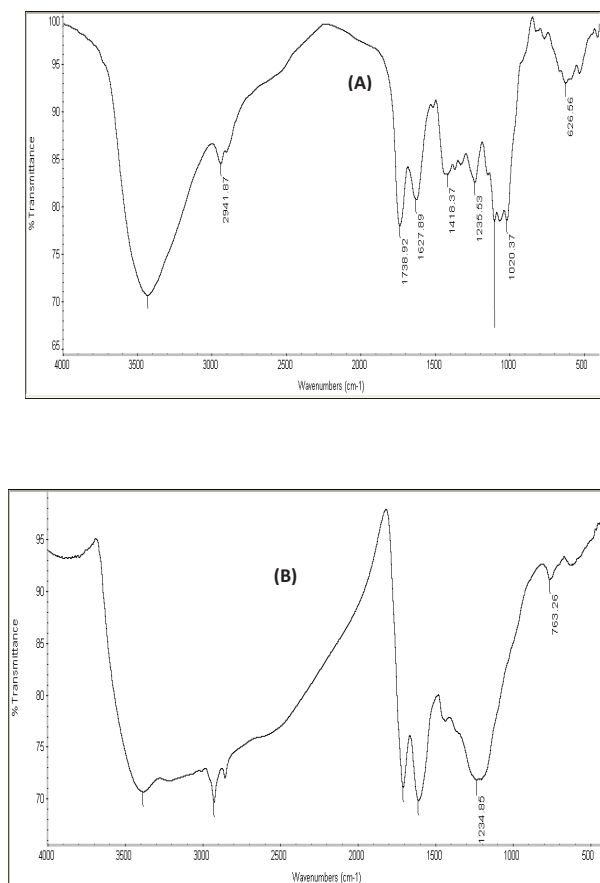

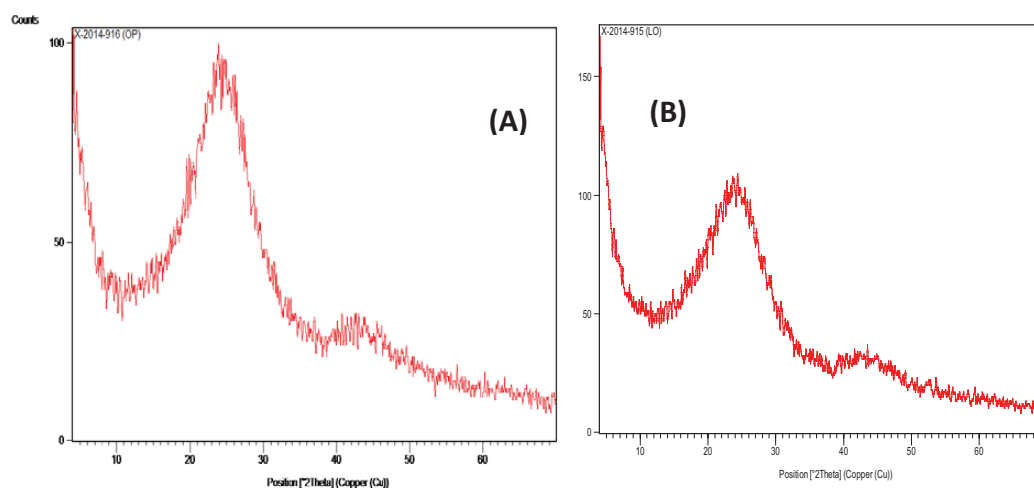Fig. 4. FTIR spectra of (A) ASAC and (B) OPAC.
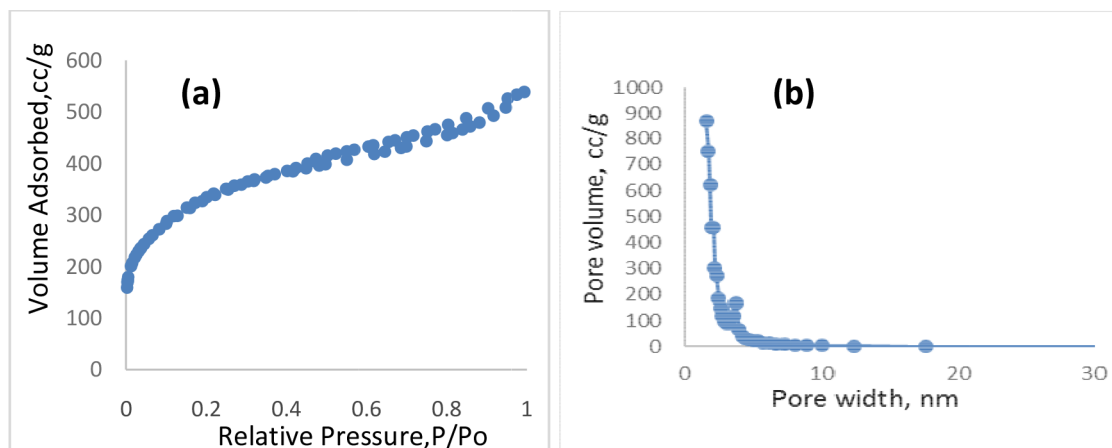

Fig. 5. XRD patterns of (A) OPAC and (B) ASAC.

Fig. 6. (a) Nitrogen adsorption/desorption isotherms and (b) the corresponding pore size distribution curve of the ASAC.
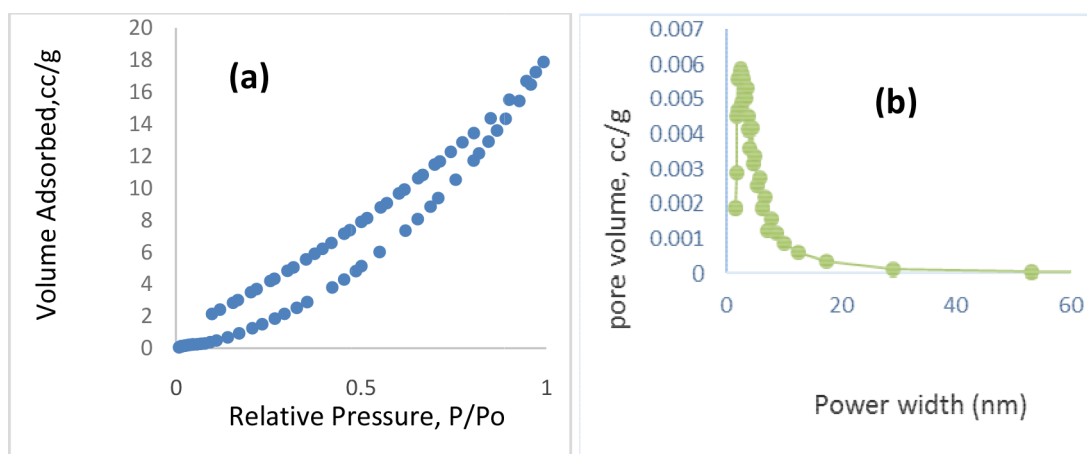

Fig. 7. (a) Nitrogen adsorption/desorption isotherms and (b) the corresponding pore size distribution curve of the OPAC.

3.2. Effect of adsorbent dose

The adsorbent dose is one of the important parameters of adsorption. It can be seen that the adsorption increases with the increase in the amount of the adsorbents. This can be explained by a greater availability of the exchangeable sites or surface area at a higher amount of the adsorbent. The adsorption percentage increases from the doses of 0.1–1 g/100 ml for OPAC and from 0.1 to 0.5 g/100 ml for ASAC. Fig. 8 shows the effect of adsorbent dose of OP and AS on the removal of acetamiprid. The optimum masses are 1 g for OPAC and 0.5 g for ASAC. The increase in adsorption capacity is probably because of the creation of some new active sites on the surface of adsorption [41].

3.3. Effect of initial concentration

The effect of initial acetamiprid concentration in the solution on the rate of adsorption onto two adsorbents (OPAC and ASAC) was studied. The experiments were carried out at fixed adsorbent dose (1 g for OPAC and 0.5 g for ASAC /100 mL) in the solution, temperature (25 ± 2°C) and at different initial concentrations of acetamiprid (100, 200, 300, 400, 500, 600, 700 and 800 mg L^{-1}). The wide range
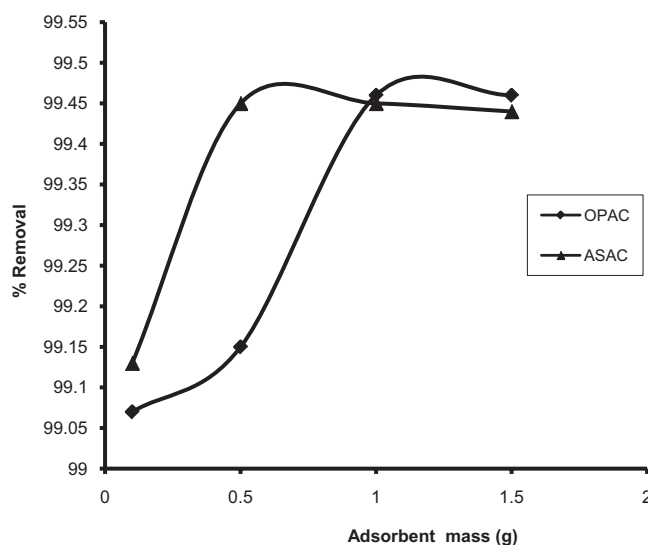

Fig. 8. Effect of different mass on removal of acetamiprid using OPAC and ASAC (initial concentration 300 mg L^{-1}, adsorbent dose 0.1–1.5 g/100 ml at room temperature).

of initial concentration of acetamiprid was used to observe the adsorption performance of acetamiprid onto two adsorbents. The results are given in Fig. 9 indicating that equilibrium adsorption capacity increases with an increase in initial concentration of acetamiprid. This reveals an increase in equilibrium adsorption capacity from 9.945 to 79.528 and 19.867 to 158.822 mg g^{-1} with increasing initial acetamiprid concentrations from 100 to 800 mg L^{-1} for OPAC and ASAC, respectively. This is probably due to the increase in the driving force of the concentration gradient. The initial acetamiprid concentration provides an important driving force to overcome all the mass transfer resistance between the solution and the solid phases.
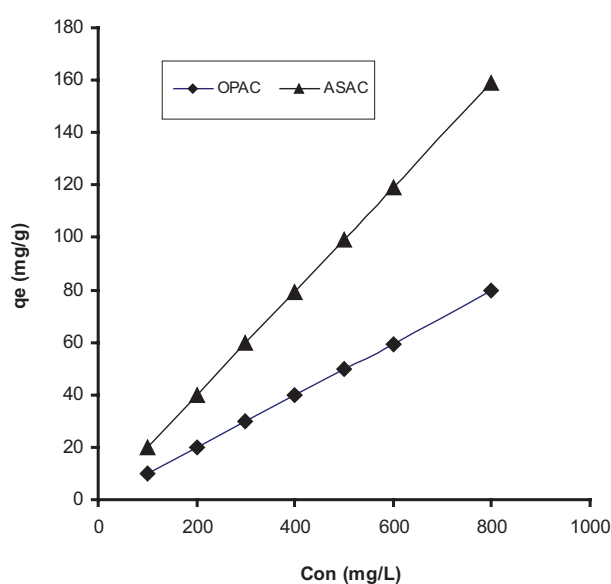

Fig. 9. Effect of initial concentration of acetamiprid (100–800 mg L^{-1}) by OPAC and ASAC.
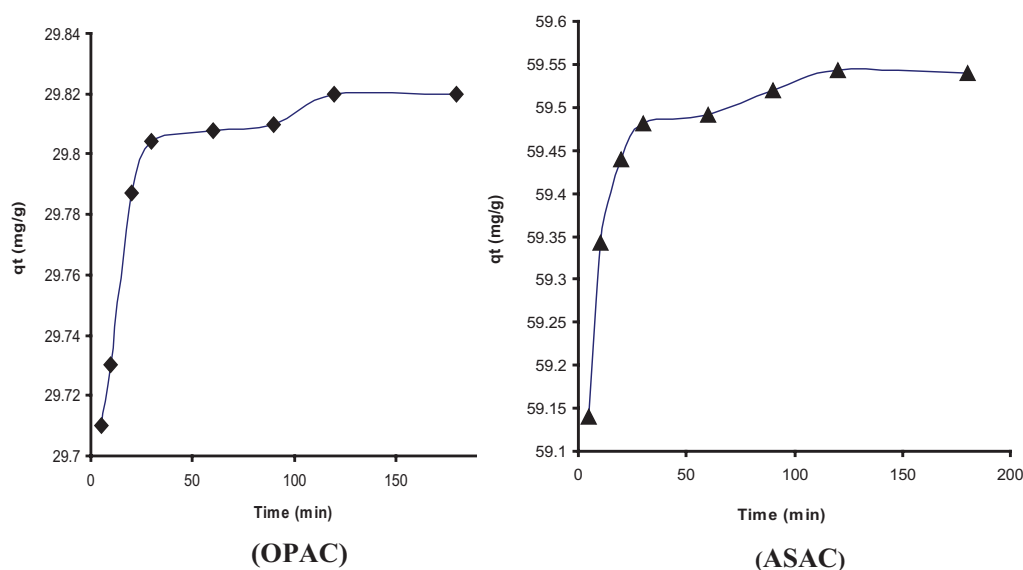
3.4. Effect of contact time

The rate at which adsorption takes place is of most important when designing batch adsorption experiments. Consequently, it is important to establish the time dependence of such systems under various process conditions. The adsorption experiments were carried out at different contact time. Fig. 10 shows the effect of contact time on the adsorption of acetamiprid with an initial concentration of 300 mg L^{-1}, adsorbent dose (1 g for OPAC and 0.5 g for ASAC), temperature (25 ± 2°C), normal pH by OPAC and ASAC at contact time 5–180 min. The pesticide adsorption rate is high for the first 30 min and finally equilibrium is established after about 120 min. The rapid pesticide adsorption at the initial stages of contact time could be attributed to the abundant availability of active sites on the surface of adsorbents. Afterwards, with the gradual occupancy of these sites, the adsorption became less efficient. Further increase in contact time did not enhance the adsorption, so, the optimum contact time for the two adsorbent was selected as 120 min for further experiments.

3.5. Biosorption kinetics

The kinetic data of the adsorption of acetamiprid onto OPAC and ASAC was evaluated using pseudo-first order and pseudo-second order kinetic models. The pseudo-first order model assumes that the rate of change of solute uptake with time is directly proportional to the difference in saturation concentration and amount of solid uptake with time. The pseudo first-order rate equation can be expressed in a linear form as:

$$\log(q_e - q_t) = \log(q_e) - \frac{K_1}{2.303}(t) \tag{3}$$

where q_e and q_t are the amount of acetamiprid adsorbed (mg g^{-1}) per unit mass of the adsorbent at the equilibrium and at time t, respectively, and k_1 is the rate constant of adsorption (min^{-1}). Values of k_1 were calculated from the plots of log (q_e

(OPAC)

(ASAC)

Fig. 10. Effect of contact time on the removal of acetamiprid by OPAC and ASAC (acetamiprid 300 mg L^{-1}).

$- q_t$) vs. t. The application of this equation to the data of acetamiprid on OPAC and ASAC (data not shown) indicated the inapplicability of the model.

The pseudo-second order model as developed by Ho and McKay [42] has the following form:

$$\frac{t}{q_t} = \frac{1}{K_2 q_e^2} + \frac{1}{q_e}(t) \tag{4}$$

where K_2 is the rate constant for the pseudo-second order kinetics (g mg⁻¹ min⁻¹). A plot of t/q_t versus time (t) would yield a line with a slope of $1/q_e$ and an intercept of $1/(k_2 q_e^2)$, if the second order model is a suitable expression. The values of K_2 and 0.4 are 1.402 and 0.47 g mg⁻¹ min⁻¹ for OPAC and ASAC, respectively. The higher value of K_2 may be attributed to the amount of adsorbent mass used (1 g).

The plot of t/q_t versus time t shows the pseudo second order model (Fig. 11). The kinetic model with a higher correlation coefficient R^2 was selected as the most suitable one (Table 2). The results show that adsorption kinetics of acetamiprid fitted well the pseudo-second-order kinetic model with a high correlation coefficient $R^2 = 1$. Similar results were also reported for the adsorption of oxamyl pesticides on different agricultural waste adsorbents [43].

3.6. Biosorption isotherms

The equilibrium isotherms are used to describe the experimental data. The adsorption isotherm is important
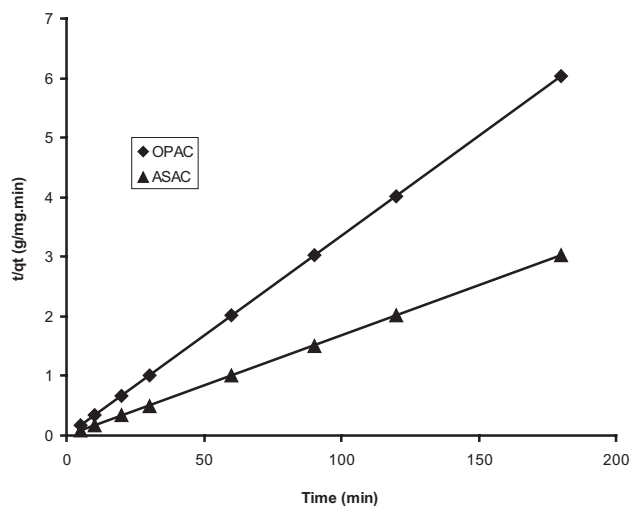

Fig. 11. Pseudo-second-order kinetic model for the removal of acetamiprid onto OPAC and ASAC.

Table 2
Kinetic parameters for the removal of acetamiprid by OPAC and ASAC

Sample	Pseudo- second order		
	K_2 (g mg⁻¹ min⁻¹)	q_e (mg g-1)	R^2
OPAC	1.402	29.850	1.000
ASAC	0.470	59.523	1.000

from both theoretical and practical point of view. To optimize the design of an adsorption system for the adsorption of adsorbates, it is important to establish the most appropriate correlation for the equilibrium curves [44]. The equation parameters of these equilibrium models often provide some insight into the sorption mechanism, the surface properties and the affinity of the adsorbent. Various isotherm equations like those of Langmuir, Freundlich, and Dubinin–Radushkevich (D–R) are the most frequently used models to describe the experimental data of adsorption isotherms.

The Langmuir isotherm assumes a surface with homogeneous binding sites, equivalent sorption energies, and no interaction between adsorbed species. Its mathematical form is written as :

$$\frac{C_e}{q_e} = \frac{1}{Q_m b} + \frac{C_e}{Q_m} \tag{5}$$

where q_e is the equilibrium metal ion concentration on the biosorbent (mg/g), b is the Langmuir constant and q_m is the monolayer adsorption capacity. The plot of C_e/q_e versus C_e is employed to generate the intercept value of $1/bq_m$ and slope of $1/q_m$ (Fig. 12).

One of the essential characteristics of this model can be expressed in terms of the dimensionless separation factor for equilibrium parameter, R_L, defined as:

$$R_L = \frac{1}{1 + bC_0} \tag{6}$$

The value of R_L indicates the type of isotherm to be irreversible ($R_L = 0$), favourable ($0 < R_L < 1$), linear ($R_L = 1$) or unfavourable ($R_L > 1$). The value of R_L in the present investigation was found to be 0.136 and 0.08 indicating that the adsorption acetamiprid onto OPAC and ASAC is favorable.

The Freundlich isotherm is an empirical equation based on an exponential distribution of adsorption sites and energies. It is represented as:

$$\log q_e = \log K_f + 1/n \log C_e \tag{7}$$

where k_F (L g⁻¹) and n are Freundlich constants related to adsorption capacity and adsorption intensity, respectively (Fig. 13). The intercept K_F obtained from the plot of $\log q_e$ versus $\log C_e$ is roughly a measure of the sorption capacity and the slope ($1/n$) of the sorption intensity (Table 3). It was indicated by that magnitude of the term ($1/n$) gives an indication of the favorability and capacity of the adsorbent/adsorbate systems [45].

Based on the correlation coefficient (R^2) shown in Table 3, the adsorption isotherms of acetamiprid on OPAC and ASAC can be slightly better described by the Freundlich equation. Similar results have been reported for the adsorption of phosphate ions by pine cone [46].

Dubinin-Radushkevich (D-R) proposed another equation used in the analysis of isotherms. D–R model was applied to estimate the porosity apparent free energy and the characteristic of adsorption [47]. The D–R isotherm do not assume a homogeneous surface or constant sorption potential and it has commonly been applied in the following form (Eq. (8)) and its linear form can be shown in Eq. (9):
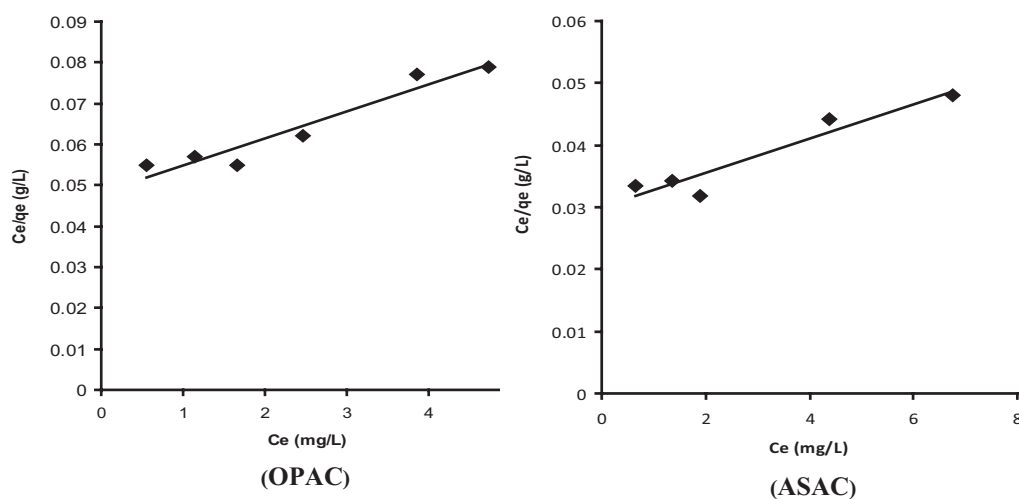
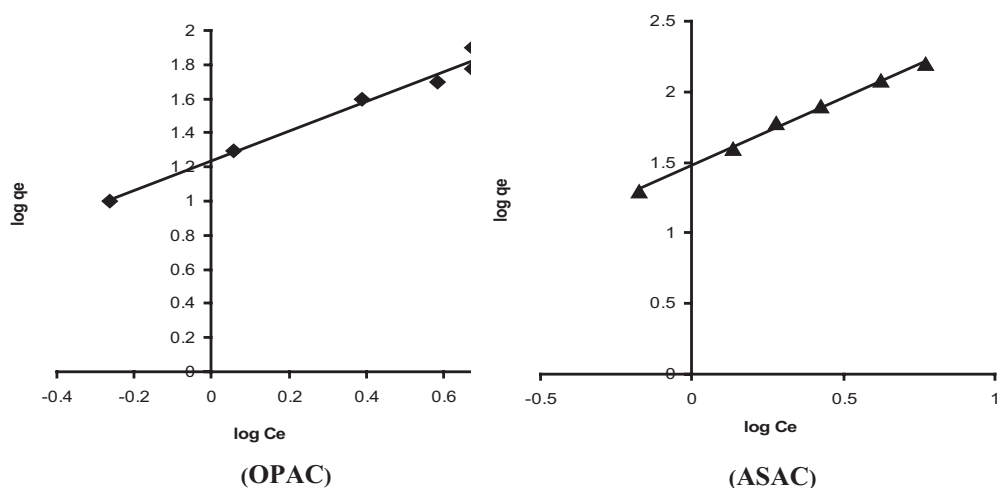Fig. 12. Langmuir isotherm for adsorption of acetamiprid using OPAC and ASAC.

Fig. 13. Freudlich isotherm for adsorption of acetamiprid using OPAC and ASAC.

$$q_e = q_m \exp\left(-K\varepsilon^2\right) \tag{8}$$

$$\ln q_e = \ln q_m - \beta\,\varepsilon^2 \tag{9}$$

where K is a constant related to the adsorption energy, q_e (mg g^{-1}) is the amount of pesticide adsorbed per g of adsorbent and q_m represents the maximum adsorption capacity of adsorbent, β (mol^2 J^{-2}) is a constant related to adsorption energy, while ε is the Polanyi potential that can be calculated from Eq. (10):

$$\varepsilon = RT \ln\left[1 + \frac{1}{C_e}\right] \tag{10}$$

The values of β and q_m can be obtained by plotting ln q_e vs. ε^2. The mean free energy of adsorption (E, J mol^{-1}), defined as the free energy change when one mole of ion is transferred from infinity in solution to the surface of the sorbent, is calculated from the K value using the following relation (Eq. (9)):

Table 3
Adsorption isotherm parameters for the adsorption of acetamiprid by OPAC and ASAC

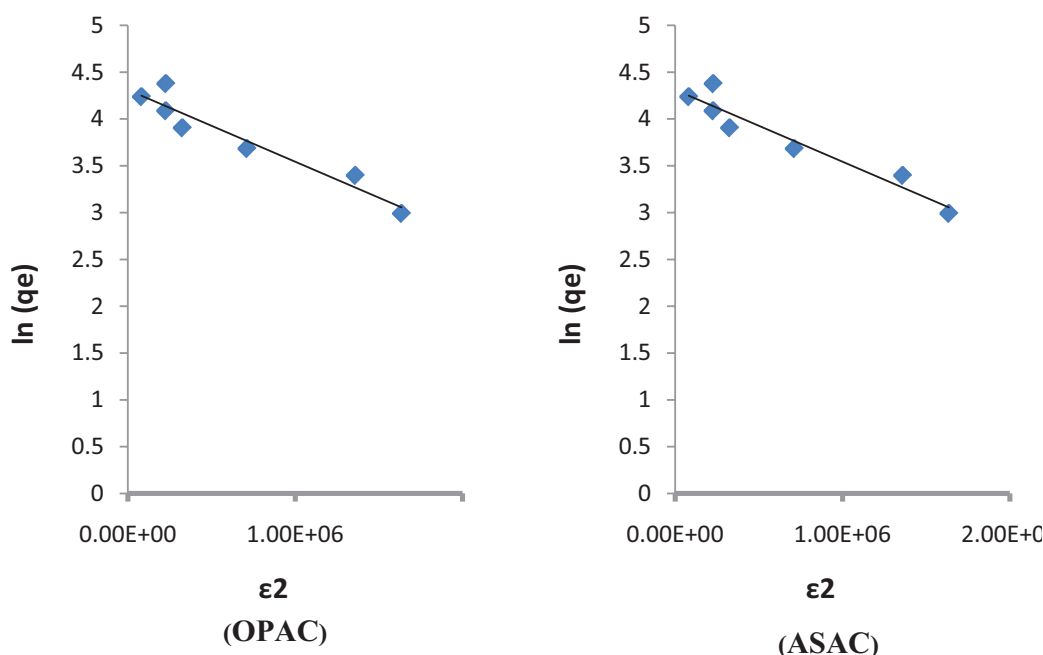| Sample	Freundlich			Langmuir			D-R		
	K_f	$1/n$	R^2	q_{max} (mg g^{-1})	b (L mg^{-1})	R^2	q_m (mg g^{-1})	E (KJ mol^{-1})	R^2
OPAC	17.186	0.873	0.9791	151.515	0.136	0.9241	74.522	0.791	0.9226
ASAC	30.18	0.958	0.9973	370.37	0.08	0.910	143.179	0.845	0.9242

Fig. 14. Dubinin- Radushkevich isotherm for adsorption of acetamiprid using OPAC and ASAC.

$$E = 1 / \sqrt{2\beta} \qquad (11)$$

The calculated values of D–R parameters are given in Fig. 14 and Table 3. The saturation adsorption capacities q_m obtained using D–R isotherm model for adsorption of acetamiprid onto OPAC and ASAC are 74.522 and 143.179 mg g^{-1}. The values of E were <8 kJ mol^{-1}, indicating that the physical adsorption process plays a significant role in the adsorption of acetamiprid onto OPAC and ASAC. These E values are in agreement with [48] for the adsorption of oxamyl onto Egyptian Apricot Stone, and for the adsorption of dyes by loofa activated carbon [49].

4. Mechanism of adsorption

The mechanism of the adsorption of acetamiprid pesticide onto two different activated carbon (Almond shells and Orange Peels) can be discussed according to the structure of acetamiprid contains aromatic rings increases the possibility of such interactions due to delocalized π electrons over the ring. Also, the presence of the branched substituent on the aromatic ring increased the level of adsorption of pesticide. The similar trend was observed by [50].

5. Conclusion

The two materials of activated carbons, orange peels (OPAC) and almond shells (ASAC) were used in this study as low cost eco-friendly agriculture waste adsorbents have been prepared.

A promising outcome based on experiments shows that orange peels and almond shells could be used as an alternative and low-cost biosorbent for removal of acetamiprid from aqueous solutions when suitable conditions are performed. The adsorption process was attained an equilibrium within 120 min of contact time. Equilibrium and kinetic studies were made for the adsorption of acetamiprid from aqueous solutions onto OPAC and ASAC. Different kinetic models are used to fit the experimental data. The Kinetic studies of the equilibrium data showed that the pseudo-second order model best describes the adsorption of acetamiprid onto the OPAC and ASAC adsorbents.

References

[1] D.L. Becker, S.C. Wilson, Carbon adsorption Handbook In: Chereminisoff, P. N., Ellebush, F. Ann Harbor Science Publishers, Michigan. The use of activated carbon for the treatment of pesticides and pesticidal wastes. Ann Harbor Science Publishers, Michigan. (1980); 167–212.

[2] A. Kouras, A. Zouboulis, C. Samara, T. Kouimtzis, Removal of pesticides from aqueous solution by combined physico chemical process-the behavior of lindane, Environ. Pollut., 103 (1998) 193–202.

[3] E. Ayrancı, N. Hoda, Adsorption kinetics and isotherms of pesticides onto activated carbon cloth, Chemosphere, 60 (2005) 1600–1607.

[4] H. Shi, G. Zhao, M. Liu, T.C. Cao, Aptamer-based colorimetric sensing of acetamiprid in soil samples: sensitivity, selectivity and mechanism, J. Hazard. Mater., 260 (2013) 754–761.

[5] L. Li, X. Chen, D.Y. Zhang, Effects of insecticide acetamiprid on photosystem II (PSII) activity of Synechocystissp (FACHB-898), J. Pesticide Biochem. Physiol., 98(2) (2010) 300–304.

[6] H.X. Yang, X. Wang, J. Zheng, G.L. Wang, Biodegradation of acetamiprid by Pigmentiphaga sp.D-2 and the degradation pathway, Inter. Biodet. Biodeg. J., 85 (2013) 95–102.

[7] M. Uğurlu, M.H. Karaoğlu, TiO$_2$ supported on sepiolite: preparation, structural and thermal characterization and catalytic behaviour in photocatalytic treatment of phenol and lignin from olive mill wastewater, Chem. Eng. J., 166 (2011) 859–867.

[8] J. Gong, C. Yang, W. Zhang, Liquid phase deposition of tungsten doped TiO$_2$ films for visible light photoelectrocatalytic degradation of dodecyl benzenesulfonate, Chem. Eng. J., 167 (2011) 190–197.

[9] H. Katsumata, T. Kobayashi, S. Kaneco, T. Suzuki, K. Ohta., Degradation of linuron by ultrasound combined with photo-Fenton treatment, Chem. Eng. J., 166 (2011) 468–473.

[10] T. Zhou, T.T. Lim, S.S. Chin, A.G. Fane, Treatment of organics in reverse osmosis concentrate from a municipal wastewater reclamation plant: feasibility test of advanced oxidation processes with/without pretreatment, Chem. Eng. J., 166 (2011) 932–939.

[11] M.I. Maldonado, S. Malato, L.A. Perez-Estrada, W. Gernjak, I. Oller, X. Domenech, Partial degradation of five pesticides and an industrial pollutant by ozonation in a pilot-plant scale reactor, J. Hazard. Mater., 38 (2006) 363–369.

[12] S.E. Gamal, I.N. Nasr, S.M. Ayman, S.G.M. Mohammad, Kinetics and thermodynamics of adsorption of cadusafos on soils, J. Hazard. Mater., 172 (2009) 1608–1616.

[13] G.M. Somaia, Biosorption of pesticide onto a low cost carbon produced from Apricot Stone (*Prunus armeniaca*).: Equilibrium, kinetic and thermodynamic studies, J. App. Sci. Res., 9(10) (2013) 6459–6469.

[14] M.K. Rai, B.S. Giri, Y. Nath, H. Bajaj, S. Soni, R.P. Singh, R.S. Singh, B.N. Rai, Adsorption of hexavalent chromium from aqueous solution by activated carbon prepared from almond shell: kinetics, equilibrium and thermodynamics study, J. Water Supply: Res. Technol., (2018).

[15] B. Munmun, K.B. Ranjan, K.D. Sudip, Cr(VI) adsorption by a green adsorbent walnut shell:adsorption studies, regeneration studies, scale-up design and economic feasibility, Process Safety Environ. Protect., (2018).

[16] N.J. Suyog, R.G. Parag, Efficient removal of Acid Green 25 dye from wastewater using activated Prunus Dulcis as biosorbent: Batch and column studies, J. Env. Manage., 210 (2018) 226–238.

[17] L. Hamza, K. Aissa, B. Badreddine, T. Mohamed, The use of prepared activated carbon as adsorbent for the removal of orange G from aqueous solution, Microchem. J., (2018) In press, accepted manuscript.

[18] A. Mittal, J. Mittal, A. Malviya, V.K. Gupta, Removal and recovery of Chrysoidine Y from aqueous solutions by waste materials, J. Colloid Interface Sci., 344 (2010) 497–507.

[19] A. Mittal, J. Mittal, A. Malviya, D. Kaur, V.K. Gupta, Decoloration treatment of a hazardous triarylmethane dye, Light Green SF (Yellowish) by waste material adsorbents, J. Colloid Interface Sci., 342 (2010) 518–527.

[20] I.A.W. Tan, A.L. Ahmad, B.H. Hameed, Adsorption of basic dye using activated carbon prepared from oil palm shell: batch and fixed bed studies, Desalination, 225 (2008) 13–28.

[21] C. Michailof, G.G. Stavropoulos, C. Panayiotou, Enhanced adsorption of phenolic compounds, commonly encountered in olive mill wastewaters, on olive husk derived activated carbons, Bioresour. Technol., 99 (2008) 6400–6408.

[22] A.A. El-Hendawy, A.J. Alexander, R.J. Andrews, G. Forrest, Effects of activation schemes on porous, surface and thermal properties of activated carbons prepared from cotton stalks, J. Anal. Appl. Pyro., 82 (2008) 272–278.

[23] J.T. Matheickal, Q. Yu, G.M. Woodburn, Biosorption of cadmium (II) from aqueous solutions by pre-treated biomass of marine alga *Durvillaea potatorum*, J. Water Res., 33 (1999) 335–342.

[24] Y.P. Ting, I.G. Prince, F. Lawson, Uptake of cadmium and zinc by the alga *Chlorella vulgaris* (II): Multi-ion situation, J. Biodet. Biodeg., 37 (1991) 445–455.

[25] S. Liang, X. Guo, N. Feng, Q. Tian, Adsorption of Cu^{2+} and Cd^{2+} from aqueous solution by mercapto-acetic acid modified orange peel, Colloids Surfaces. B: Biointerfaces, 73 (2009) 10–14.

[26] S. Liang, X. Guo, N. Feng, Q. Tian, Application of orange peel xanthate for the adsorption of Pb^{2+} from aqueous solutions, J. Hazard. Mater., 170 (2009) 425–429.

[27] M.R. Mehrasbi, Z. Farahmandkia, B. Taghibeigloo, A. Taromi, Adsorption of lead and cadmium from aquous solution by using almond shell, Water Air Soil Pollution, 199 (2009) 343–351.

[28] D. Ozdes, A. Gundogdu, C. Duran, H.B. Senturk, Evaluation of adsorption characteristics of malachite green onto almond shell (Prunus dulcis), Sep. Sci. Tech., 45 (2010) 2076–2085.

[29] M. Sahranavard, A. Ahmadpour, M.R. Doosti, Biosorption of hexavalent chromium ions from aqueous solutions using almond green hull as a low cost biosorbent, Eur. J. Sci. Res., 58(3) (2011) 392–400.

[30] A.J. Esfahlan, R. Jamei, R.J. Esfahlan, Food Chemistry, 120 (2010) 349–360.

[31] Z. Ch Fatima, B. Belkacem, Removal of acetamiprid from aqueous solutions with low-cost sorbents, Desal. Water Treat., 58 (2016) 419–430.

[32] V.O. Njoku, B.H. Hameed, Preparation and characterization of activated carbon from corncob by chemical activation with H$_3$PO$_4$ for 2,4-dichlorophenoxyacetic acid adsorption, Chem. Eng. J., 173 (2011) 391–399.

[33] F.N. Arslanoglu, F. Kar, N. Arslan, Adsorption of dark coloured compounds from peach pulp by using powdered activated carbon, J. Food Eng., 71 (2005) 156–163.

[34] H. Saeedeh, S. Khatereh, A.Y. Zahra, Preparation of activated carbon from agricultural wastes (almond shell and orange peel) for adsorption of 2-pic from aqueous solution, J. Ind. Eng. Chem., 20 (2014) 1892–1900.

[35] P.K. Chayande, S. P. Singh, M.K.N. Yenkie, Characterization of activated carbon prepared from Almond shells for Scavenging phenolic pollutants, Chem. Sci. Trans., 2(3) (2013) 835–840.

[36] Y.S. Ho, G. McKay, D.A.J. Wase, C.F. Foster, Study of the sorption of divalent metal ions on to Peat, Ads. Sci. Tech., 18 (2000) 639–650.

[37] M.S. Mahmoud, M.A. Sahar, G.M. Somaia, M.A. Ahmed, Evaluation of Egyptian banana peel (*Musa* sp.) as a green sorbent for groundwater treatment, Int. J. Eng. Tech., 4(11) (2014).

[38] Z. Chen, F. Shan, L. Cao, G. Fang, Synthesis and thermal properties of shape-stabilized lauric acid/activated carbon composites as phase change materials for thermal energy storage, Solar Energy Mater, Solar Cells, 102 (2012) 131–136.

[39] K. Kumar, R.K. Saxena, R.D. Kothari, K. Suri, N.K. Kaushik, J.N. Bohra, Correlation between adsorption and x-ray diffraction studies on viscose rayon based activated carbon cloth, Carbon, 35(12) (1997) 1842–1844.

[40] H. Xiuli, J. Haixia, Z. Yong, H. Weifeng, Z. Yangfan, G. Ping, D. Rui, L. Enhui, A high performance nitrogen-doped porous activated carbon for supercapacitor derived from pueraria, J. Alloys Comp., 744 (2018) 544–551.

[41] S.H. Chen, J. Zhang, C.L. Zhang, Q.Y. Yue, Y. Li, C. Li, Equilibrium and kinetic studies of methyl orange and methyl violet adsorption on activated carbon derived from Phragmites australis, Desalination, 252 (2010) 149–156.

[42] Y.S. Ho, G. McKay, D.A.J. Wase, C.F. Foster, Study of the sorption of divalent metal ions on peat, Ads. Sci. Tech., 18 (2000) 639–650.

[43] S.G. Mohammad, S.M. Ahmed, A.M. Badawi, A comparative adsorption study with different agricultural waste adsorbents for removal of oxamyl pesticide, Desal. Water Treat., 55 (2015) 2109–2120.

[44] A. Altinisik, E. Gur, Y. Seki, A natural sorbent, Luffa Cylindrical for the removal of a model basic dye, J. Hazard. Mater., 179(1–3) (2010) 658–664.

[45] V.J.P. Poots, G. McKay, Removal of basic dye from effluent using wood as an adsorbent, J. Water Pollut. Control Fed., 50 (1978) 926–935.

[46] S. Benyoucef, M. Amrani, Adsorption of phosphate ions onto low cost Aleppo pine adsorbent, Desalination, 275 (2011) 231–236.

[47] M.M. Dubinin, Zh. Fiz. Khim, Modern state of the theory of volume filling of micropore adsorbents during adsorption of gases and steams on carbon adsorbents, Zh. Fiz. Khim., 39 (1965) 1305–1317.

[48] M.A. Sahar, G.M. Somaia, Egyptian Apricot Stone (*Prunus armeniaca*) as a low cost and eco-friendly biosorbent for oxamyl removal from aqueous solutions, Am. J. Exp. Agri., 4(3) (2014) 302–321.

[49] O. Abdelwahab, Evaluation of the use of loofa activated carbons as potential adsorbents for aqueous solutions containing dye, Desalination, (2008) 257–236.

[50] V. Marija, K. Ana, B. Biljana, L. Zoran, L. Mila, Influence of different carbon monolith preparation parameters on pesticide adsorption, J. Serb. Chem. Soc., 78(10) (2013) 1617–1632.